Progress In Electromagnetics Research B, Vol. 39, 141–161, 2012

INFLUENCE OF CELLULAR PROPERTIES ON THE ELECTRIC FIELD DISTRIBUTION AROUND A SINGLE CELL

H. Ye [1, 2, 5, *], M. Cotic [3], M. G. Fehlings [1, 4, 5], and P. L. Carlen [1, 2, 5]

[1]Toronto Western Research Institute, University Health Network, Toronto, Ontario, M5T 2S8, Canada

[2]Department of Physiology, University of Toronto, Toronto, Ontario, M5S 1A1, Canada

[3]Institute of Biomaterials and Biomedical Engineering, University of Toronto, Toronto, Ontario, M5S 1A1, Canada

[4]Department of Surgery, University of Toronto, Toronto, Ontario, M5S 1A1, Canada

[5]Neuroscience Program, University of Toronto, Toronto, Ontario, M5S 1A1, Canada

Abstract—Electric fields have been widely used for the treatment of neurological diseases, using techniques such as non-invasive brain stimulation. An electric current controls cell excitability by imposing voltage changes across the cell membrane. At the same time, the presence of the cell itself causes a re-distribution of the local electric field. Computation of the electric field distribution at a single cell microscopic level is essential in understanding the mechanism of electric stimulation. In addition, the impact of the cellular biophysical properties on the field distribution in the vicinity of the cell should also be addressed. In this paper, we have begun by first computing the field distribution around and within a spherical model cell. The electric fields in the three regions differed by several orders of magnitude. The field intensity in the extracellular space was of the same order as that of the externally applied field, while in the membrane, it was calculated to be several thousand times greater than the applied field. In contrast, the field intensity inside the cell was greatly attenuated to approximately 1/133th of the applied field. We then performed a

Received 27 December 2011, Accepted 27 February 2012, Scheduled 2 March 2012

* Corresponding author: Hui Ye (hye@uhnresearch.ca).

detailed analysis on the dependency of the local field distribution on both the electrical properties (i.e., conductivity, dielectricity), and the geometrical properties (i.e., size, membrane thickness) of the target cell. Variations of these parameters caused significant changes to the amplitude and direction of the electric field around a single cell. The biophysical mechanisms of such observations and their experimental implications are discussed. These results highlight the significance of considering cellular properties during the electric stimulation of neuronal tissues.

1. INTRODUCTION

Electric fields have been widely used to treat neurological disorders including Parkinson's disease, essential tremor and dystonia [1]. Recent research has focused on developing non-invasive magnetic and electric stimulation methods to activate/deactivate brain tissue, as it is more attractive in clinical practice and present new application possibilities [2–4].

What are the underlying mechanisms that determine the effects of electric stimulation? When neuronal tissue is positioned inside an electric field, the electric field induces a change in the resting transmembrane potential by superimposing an electrically induced potential. During this process, the neural tissue also redistributes the externally applied field, including the field around the cell, inside the cell membrane and in the cytoplasm [5, 6]. This "interaction" between the electric field and the neuronal tissue suggests that both may impact the efficacy of stimulation. Attempts to derive an expression for the transmembrane potential during electric stimulation for a single cell began as early as the 1950s [7, 8]. Later studies added more complexity to the modeled cell and provided insight into the factors affecting the induced transmembrane potential. This included both the electrical [5, 9–12] and geometrical properties of the cell, such as its shape [13, 14] and orientation to the field [15, 16]. These works stressed the importance of cellular properties in the build-up of the transmembrane potential.

The second aspect of the "cell-field interaction", (i.e., re-distribution of the local electric field by the target cell) has only been partially addressed, although several analytical works have attempted to study the field distribution around a single cell. Among these, Farkas et al. [17] provided a partial solution for the transmembrane electric field in a spherical cell model. Jerry et al. [18] solved the electric distribution inside and outside of a cell with a prolate spheroidal shape. Wachner et al. [19] provided an analytical solution to the magnitude

of the electric field at several representative points (equatorial site and polar site) on a single cell membrane. These studies have not attempted to provide and compare electric field distributions in all the macroscopic cellular regions in a single model entity, namely the extracellular space, the membrane, and the intracellular cytoplasm. Moreover, the basic modeling setup varies among different models. For example, some models assume that the membrane is non-conductive, while others assume that the membrane is low-conductive. These inconsistencies, among different modeling approaches, also prevent a detailed comparison of local field distributions in all the regions.

At a microscopic cellular level, the electric field around a cell is separated into three major components by the low conductive cell membrane: the field in the extracellular medium (i.e., extracellular field), within the membrane (transmembrane field), and in the cytoplasm (intracellular field). Many important cellular physiological processes are associated with these fields. In the extracellular space, interneuronal communication via ephaptic interactions has been observed to facilitate synchronized and even epileptic-like neuronal bursting [20], and epileptogenesis [21]. Computing extracellular electric fields has been a major task in various modeling works studying the electric excitation of nerve tissues [22–24]. The transmembrane electric field maintains the meta-stable membrane structure [25], and is essential for the manipulation of the transmembrane potential during electroporation [26]. Finally, the electric field that penetrates into the cytoplasmic space (intracellular field) is likely important in polarizing internal organelles such as mitochondria [14] and in facilitating polynucleotide uptake and migration within the cell [27]. In order to make a direct comparison of electric fields within these three regions, our first goal in this paper is to provide analytical solutions for the electric fields in the extracellular space, within the cell membrane and inside the target cell.

Previous studies have also attempted to understand the importance of cellular properties on the field distributions during electric stimulation. At present, the impact of only two cellular properties, the gross tissue conductivity [28] and the membrane resistance [29, 30], have been investigated with numerical methods. The impact of other cellular properties, including geometric properties (i.e., cell radius and membrane thickness) and electrical properties (i.e., conductivities of the extracellular medium, and the cytoplasm), are largely unknown. Using the derived analytical solutions for the electric field distributions, the second goal of this paper is to investigate the effects of these cellular properties on the local field distribution around the cell. These results highlight the significance of considering cellular

properties during the electric stimulation of neuronal tissues. The experimental implications of such analyses are also discussed.

2. METHODS

Several assumptions were made in setting up the model and selecting the model parameters. This was done to reduce computational complexity, while still maintaining a given level of biological relevance for the model. As illustrated in Figure 1, we modeled the cell as a spherical membrane shell (1#) with extracellular medium (0#) and intracellular cytoplasm (2#). The center of the cell was at point O. To simplify calculations, we assumed that each region was homogenous and isotropic with electric conductivities σ_0, σ_1, σ_2. The inner and outer radii of the membrane were R_- and R_+, respectively. The membrane thickness was $d = R_+ - R_-$. The cell was exposed to a uniform external field $\vec{E} = E\vec{Z}$, where $\vec{Z}$ is the unitary vector in the direction of the external field. We derived expressions for the potentials in the extracellular medium, the membrane, and the cytoplasm by solving Laplace's equation $\nabla^2 V = 0$ with appropriate boundary conditions, because these domains are source-free. The electric field distributions in all regions were calculated as $\vec{E} = -\nabla V$, where V is the potential. Four boundary conditions were considered in solving Laplace's equation. (1) The potential and (2) the normal components of the current density are continuous across the boundary of two different media, i.e., between cytoplasm/membrane interface

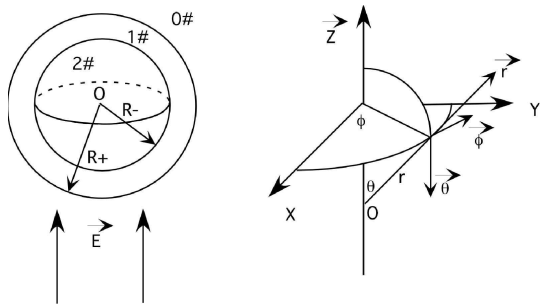

Figure 1. The spherical cell model and the spherical coordinate system (r, θ, ϕ) The cell includes three homogenous, isotropic regions: the extracellular medium, the membrane and the cytoplasm. The externally applied DC electric field is in spherical coordinates (r, θ, ϕ). The axis of the electric field overlaps with the OZ axis.

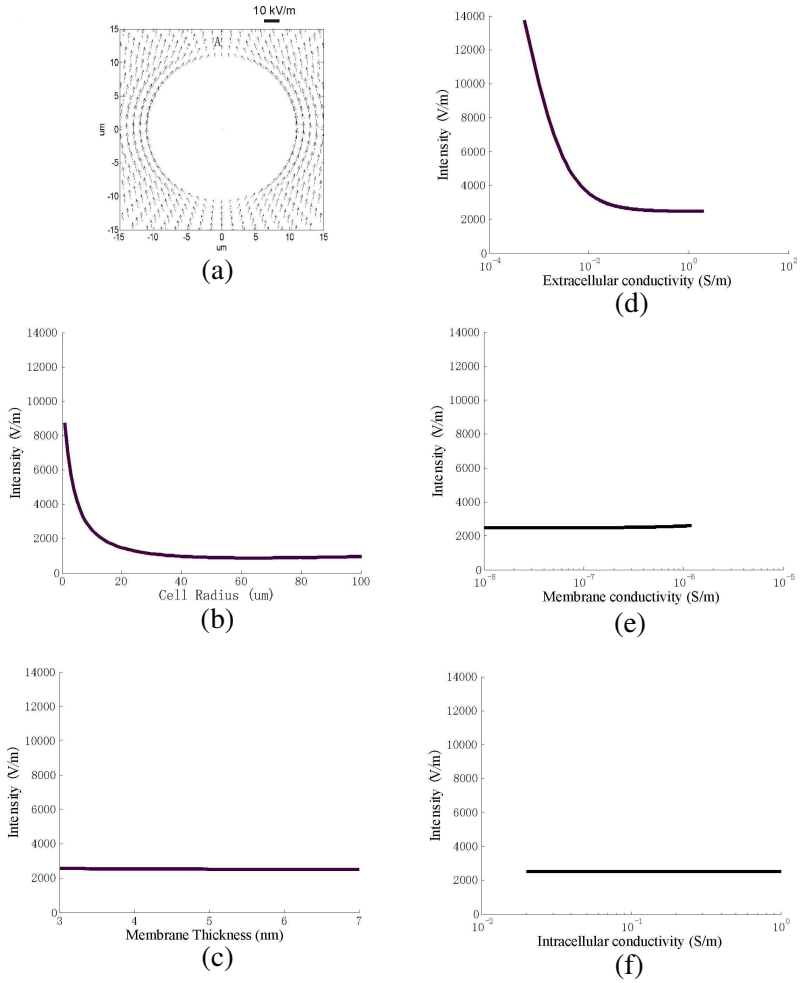

Figure 2. Dependency of the extracellular electric field on the geometrical and electrical properties of the cell. (a) Extracellular electric field around the cell in the y-z plane as shown in Figure 1. The electric field detours around the cell membrane. The electrical field intensity of a point (A) that is 1 µm away from the membrane in the extracellular space was examined. (b) Impact of cell radius on the extracellular field intensity. (c) Impact of membrane thickness on the extracellular field intensity. (d) Impact of extracellular conductivity on the extracellular field intensity. (e) Impact of membrane conductivity on the extracellular field intensity. (f) Impact of intracellular conductivity on the extracellular field intensity.

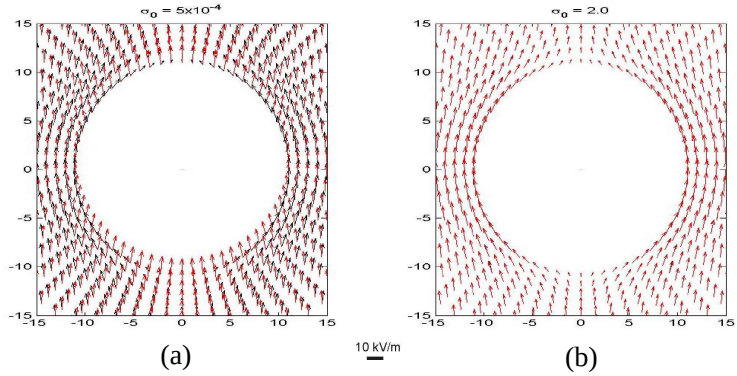

Figure 3. Effect of the extracellular conductivity on the direction of the electric field in the extracellular medium. For direct comparison, the electric field corresponding to the standard value (0.2 S/m) is illustrated by black arrows, and the electric field corresponding to the specified extracellular conductivities is illustrated by red arrows. (a) Extracellular conductivities of 5×10^{-4} S/m (red) versus 0.2 S/m (black). (b) Extracellular conductivities of 2.0 S/m (red) versus 0.2 S/m (black).

and membrane/extracellular medium interface; (3) the electric field at an infinite distance from the cell is not perturbed by the presence of that cell; and (4), the potential inside the cell is finite. The intensities of the electric fields in the three regions were studied by choosing a representative point in each region. Point A is on the geometrical pole closest to the cathode electrode and just outside the cell membrane (Figure 2(a)). Point B is on the membrane pole (Figure 4(a)), point O is at the center of the cell (Figure 5(a)).

Model parameters were adapted from a previous publication [9]. These include the geometrical and electrical parameters of the cell and their respective standard physiological values, defined by lower and upper limits (Table 1). The intensity of the external field was chosen to be 10000 V/m [30, 31]. This allowed for a maximum of several hundred mV of polarization, as used in typical electroporation experiments.

3. RESULTS

3.1. Electric Field Distribution

A detailed derivation of the expressions for the electric fields in the extracellular space surrounding the cell, inside the membrane, and in

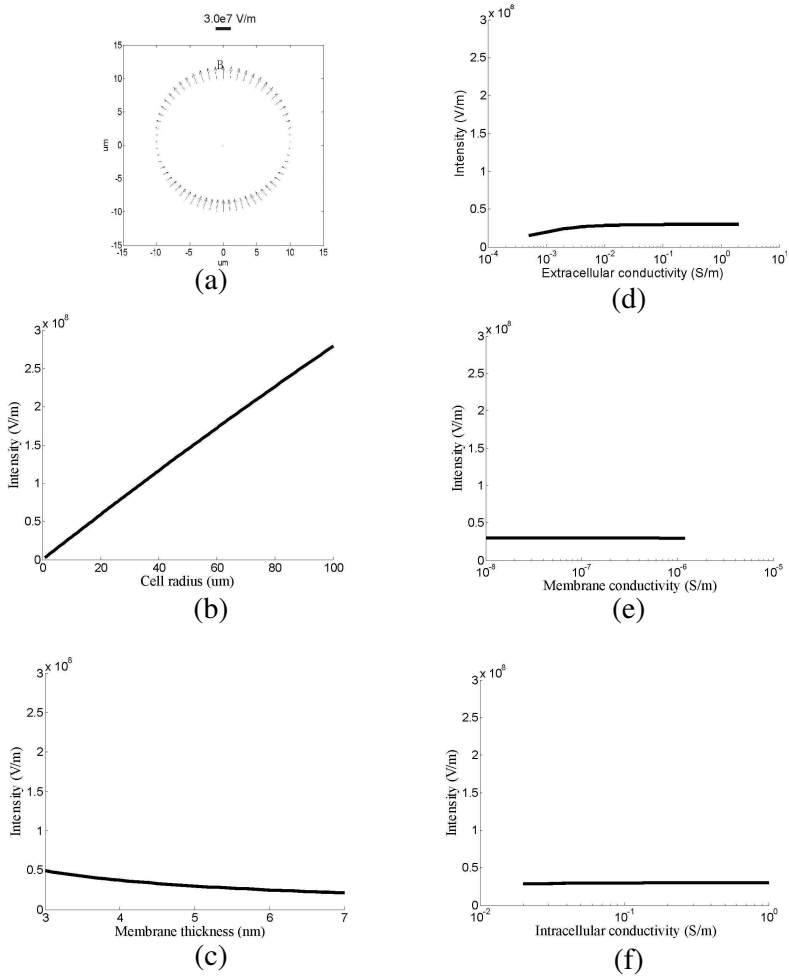

Figure 4. Dependency of the transmembrane electric field on the geometrical and electrical properties of the cell. (a) Transmembrane electric field distribution in the *y*-*z* plane as in Figure 1. The electric field is perpendicular to the cell membrane. The electrical field intensity of a point (B) inside the membrane was examined. (b) Impact of cell radius on the transmembrane field intensity. (c) Impact of membrane thickness on the transmembrane field intensity. (d) Impact of extracellular conductivity on the transmembrane field intensity. (e) Impact of membrane conductivity on the transmembrane field intensity. (f) Impact of intracellular conductivity on the transmembrane field intensity.

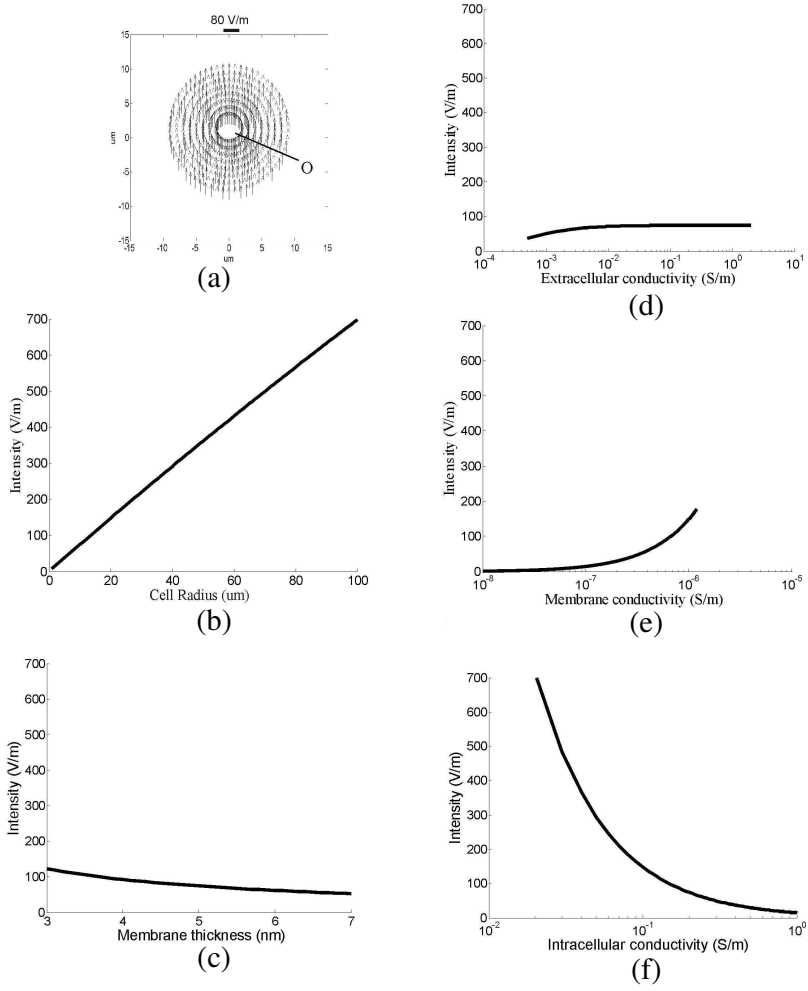

Figure 5. Dependency of the intracellular (cytoplasmic) electric field on the geometrical and electrical properties of the cell. (a) Intracellular electric field distribution in the y-z plane as in Figure 1. The electric field everywhere inside the cell is in the same direction as the externally applied field. The electrical field intensity of a point (O) at the center of the cell was examined. (b) Impact of cell radius on the intracellular field intensity. (c) Impact of membrane thickness on the intracellular field intensity. (d) Impact of extracellular conductivity on the intracellular field intensity. (e) Impact of membrane conductivity on the intracellular field intensity. (f) Impact of intracellular conductivity on the intracellular field intensity.

Table 1. Model parameters.

Parameters	Lower limit	Standard value	Upper limit
Extracellular conductivity (σ_0, S/m)	5×10^{-4}	0.2	2.0
Membrane conductivity (σ_1, S/m)	1.0×10^{-8}	5×10^{-7}	1.2×10^{-6}
Cytoplasmic conductivity (σ_2, S/m)	2.0×10^{-2}	0.2	1.0
Cell radius (R, μm)	5	10	20
Membrane thickness (d, nm)	3	5	7

the cytoplasm, is shown in the Appendix. Figures (2a), (4a) and (5a) illustrate these electric field distributions using standard values listed in Table 1 and Equations (A19)–(A27). Due to the symmetry of the solutions to ϕ, we plotted the electric distribution in a 2D plot that represents the y-z plane.

The electric fields in the three regions differed by several orders of magnitude. With the standard values listed in Table 1, the intensity was 2531.6 V/m in the extracellular space (point A), which was comparable with that of the externally applied field. The maximal field intensity in the membrane was 2.98×10^7 V/m (point B), which was several thousand times greater than the applied field. The electric field intensity inside the cell was greatly attenuated to about 1/133th of the applied field, with a value of 74.5 V/m in the center of the cell (point O). The dramatic differences between the membrane field and extra/intra fields are quantitatively in agreement with that suggested previously [19] for these representative points. The intensities of the electric fields in all three regions (extracellular vicinity, membrane, and intracellular space) were linearly proportional to the intensity of the externally applied field (E). However, the sensitivities of the electric fields to the parameters that define the geometrical properties (cell radius R and membrane thickness d) and electrical properties of the cell ($\sigma_0,\ \sigma_1,\ \sigma_2$) were more complicated, as discussed below.

3.2. Sensitivity of the Extracellular Electric Field to the Geometrical and Electrical Parameters of the Cell

Equations (A19)–(A21) suggest that the distribution of the extracellular electrical field close to the cell attenuates as a function of $1/r^3$, where r is the distance between a point in the extracellular space to the center of the cell. This rapid drop-off with distance suggests that although the presence of the cell affects the field distribution [5], its effect is more pronounced near the cell (Figure (2a)). We analyzed the electrical field intensity at point A. Between the two geometrical parameters that were considered, the cell radius had a greater impact on the field intensity at this point. Figure 2(b) shows that an increase in cell size was associated with a decrease in the electric field, and this decrease was most obvious when the cell size changes within the range of 1–20 μm. When the cell radius was greater than 20 μm, the field intensity became insensitive to the cell radius. The membrane thickness had a trivial effect on the extracellular electric field intensity (Figure 2(c)).

Among the three electrical parameters considered in the model, the extracellular conductivity had the largest impact on the field intensity at point A. As shown in Figure 2(d), an increase in the extracellular medium conductivity (in its lower physiology range, $< 10^{-2}$ S/m) lead to a significant decrease in the field intensity. The extracellular field intensity was less sensitive to the extracellular conductivity at its higher physiological range ($> 10^{-2}$ S/m). An increase in the extracellular conductivity also had an interesting impact on the direction of the electric field proximal to the outer membrane; the electric field tended to flow along the membrane rather than penetrate through the membrane in a high conductive medium (Figure 3). Compared with the significant impact of the extracellular conductivity on the field intensity, increases in membrane conductivity (Figure 2(e)) or cytoplasmic conductivity (Figure 2(f)) only lead to small ($< 5\%$) increases in the extracellular field intensity.

3.3. Sensitivity of the Transmembrane Electric Field to the Geometrical and Electrical Parameters of the Cell

The transmembrane electric field was several orders greater than those inside/outside the cell, as if it had been "magnified". This feature results from extremely low membrane conductivity, and the boundary condition (2), which states that the normal component of the current density is continuous across the membrane/extracellular medium interface. Therefore, during electric stimulation, a large amount of energy will target the membrane system of the biological tissue. As

E_{1r} was several orders greater than $E_{1\theta}$, the transmembrane electric field was approximately perpendicular to the membrane everywhere inside the membrane (Figure 3(a)). The transmembrane electric field was maximal at the two poles corresponding to $\theta = 0^\circ$ and $\theta = 180^\circ$, respectively. On the equator ($\theta = 90^\circ$), the electric field was parallel to the membrane surface and nearly zero, since the large magnitude component of E_{1r}, is zero. Figure 4(b) shows that the transmembrane electrical field was strongly dependent on the cell radius. An increase in cell size caused an approximately linear increase in the transmembrane electrical field. An increase in membrane thickness caused a small decrease in transmembrane field intensity (Figure 4(c)). An increase in extracellular conductivity caused a small, but noticeable increase in the transmembrane electrical field, especially at lower physiological values (Figure 4(d)). An increase in membrane conductivity caused a trivial decrease in transmembrane electrical field intensity (Figure 4(e)), which is in agreement with a previous study [30] using a numerical approach. Finally, increases in cytoplasmic conductivity caused trivial increases in transmembrane electrical field intensity (Figure 4(f)) in the parameter range considered.

3.4. Sensitivity of the Intracellular Electric Field to the Geometrical and Electrical Parameters of the Cell

The intracellular electric field was several orders smaller than that of the extracellular medium. When the membrane was considered non-conductive, the electric field inside the cell was nullified by induced charges at the surface of the cytoplasm. The intracellular electric field maintained the same direction as the external field everywhere inside the cell (Figure 5(a)). While a larger cell size was associated with a greater intracellular field intensity (Figure 5(b)), an increase in membrane thickness caused a decrease in field intensity (Figure 5(c)). The intracellular electric field intensity was most sensitive to the extracellular conductivity at lower physiological values ($< 10^{-2}$ S/m). An increase in extracellular conductivity within this range slightly increased the intracellular electrical field intensity. At high physiological values ($> 10^{-2}$ S/m), the intracellular electrical field intensity was less sensitive to the change in extracellular conductivity. An increase in membrane conductivity enhanced the electric field intensity in the intracellular space (Figure 5(e)), and this enhancement was most obvious when the extracellular conductivity was at higher physiological values ($> 10^{-7}$ S/m). This result is in accordance with the idea that a more conductive membrane allows fields to penetrate into the cell. Finally, an increase in cytoplasmic conductivity caused a decay in the intracellular field intensity (Figure 5(f)).

4. DISCUSSION

The objective of this study was to investigate how cellular properties influence the electrical field distribution around a single model cell, under DC electric stimulation. Here, we have provided the first full analytical expressions of the field distributions around the cell. Furthermore, we have provided a complete analysis of the electrical and geometrical cellular parameters of this traditional spherical cell model, and their impact on the electric field distributions inside and outside the cell and within the membrane.

4.1. Electric Field Distribution around a Single Cell

In agreement with previous works [5, 6], this study demonstrates that the presence of the cell leads to a redistribution of the local field around the cell. An electric field perturbed by one cell could have a secondary effect on neighboring cells. Simulation work has demonstrated that if two cells are located close to each other, they interact and alter each other's patterns and amounts of polarization, through perturbation of the extracellular electrical field [32, 33]. Experimental work has also provided supportive evidence for such conclusions. Using imaging techniques, it has been observed that large clusters of cells demonstrated complex polarization behaviors [34] during electric field stimulation, a consequence of a secondary effect due to field distortion by neighboring cells. Although an analytical solution for such "cell-cell interaction" is not yet available, our analysis suggests two important aspects of such an interaction. First, it may only exist in a high-density cell medium, since the perturbation of the extracellular electric field attenuates as a function of $1/r^3$ (Figure 2(a)), which is a very fast decay. Second, it may depend on the electrical and geometrical properties of the cells, as studied in this paper. Therefore, the effects of cellular properties should be considered when studying cell-cell interactions between neighboring cells during electric field stimulation.

We have provided an expression for the transmembrane electric field (A25) in this paper. A previous study [17] provided a solution that is similar to equation (A25), which the authors named "intramembrane field intensity". Unlike us, the authors did not consider the $E_{1\theta}$ and $E_{1\phi}$ components in their solution. In this work, we confirmed that both the $E_{1\theta}$ and $E_{1\phi}$ components could be ignored only if one assumes that the cell membrane is non-conductive. Therefore, (A25) is a more complete expression for the electric field inside the membrane for the spherical cell model. Several studies have shown that the field that penetrates into the cell is greatly attenuated due to the extremely low membrane conductivity [5, 18]. Equations (A28)–(A30) in this work

confirm such observations. It has also been shown that the intracellular field is uniform across the intracellular space [18]. This work provides the mathematical basis for such homogeneity of the intracellular field distribution. In Equations (A28)–(A30), E_{2r} contains the $\cos\theta$ term and $E_{2\theta}$ contains the $\sin\theta$ term. These terms were canceled out when computing the total electric field, and the overall intracellular electric field became independent of θ.

4.2. Implication of Cellular Properties on Electric Stimulation

During electric stimulation, electrical charges accumulate on the two interfaces that define the inner and outer sides of the cell membrane (i.e., the extracellular medium/outer membrane interface and the inner membrane/cytoplasm interface). This ensures the non-zero solution of the transmembrane potential and electric field. Therefore, field re-distribution is an intrinsic feature to any tissue with non-homogenous properties.

This work shows that electric fields are highly dependent on cellular properties, suggesting that aside from changing the field, modifying these properties may alter the effects of electric stimulation [35]. It has been suggested [36] that the anisotropic nature of the tissue surrounding the stimulated nucleus might affect the shape of the electric field and in turn neural polarization. A recent work [30] studied the intracellular electric field under uniform electric field stimulation using numerical analysis. The authors focused on the impact of the membrane resistance over a wide range of values, on the intracellular field, and found that the intracellular field increased greatly as membrane resistance decreased. Using the analytical solutions derived here, our model confirms this observation, as the intracellular electric field was 1.5 V/m with a low conductive membrane, compared to 176.99 V/m with a high conductive membrane. We further present evidence that the intracellular electric field is dependent on intra- and extracellular conductivities, as well as the cell radius and membrane thickness. As all these parameters are interrelated, their individual impact on the intracellular electric field may be strengthened or weakened by the changes in other parameters. Therefore, the electric field that can penetrate through the membrane is affected by cellular properties in a complex manner.

This model shows that the size of the cell affects the magnitude of the electric field around the cell. During the electric stimulation of neuronal tissues, the cell radius is a major factor that affects the stimulation threshold. For example, during deep brain stimulation, the relative magnitude of the effects of electric stimulation within different

brain regions depends on axon fiber size [37]. In electroporation, larger cells require lower external fields to create permeable cell membranes [38]. Since a larger cell is associated with a smaller extracellular electric field (Figure 2(b)), this implies that successful electroporation does not necessarily require a large local field around the cell. The build-up of the transmembrane potential and the associated change in membrane permeability should serve as better indicators for the effects of electroporation [38].

The fact that the electric field distribution is distorted on the interface of two non-homogenous materials (including biological tissue and other physical medium) has experimental implications. Currently, many researchers use invasive methods (patch and voltage clamps, microelectrodes) to measure electric field distributions during electric stimulation. The presence of these electrodes themselves may further perturb the applied field in the tissue. As such, to accurately quantify field distributions and transmembrane potential changes during electric stimulation, other less invasive methods should be considered. For example, voltage sensitive dyes that provide both high temporal and spatial resolutions have been successfully used to measure potential changes [5, 34, 39].

4.3. Future Directions

To simplify computations, several assumptions have been made to formulate the present model, which should be addressed in future studies. First, the cell is represented as a spherical shell, and this oversimplification may be biologically simple, considering that the membrane polarization induced by an applied field is dependent on the complex geometrical structure of the membrane [40]. Future work should consider multi-compartment modeling or finite element meshes [22, 23, 32] to model this geometrical complexity. Second, both the extracellular medium and cytoplasmic environment are not truly homogenous [41, 42]. Our model results suggest that varying both the intracellular and extracellular conductivities can change the electric field distribution, suggesting that if more biologically authentic electric properties of the tissue were involved in the model, the resulting electric field could be disturbed in a more complicated pattern than those shown in Figure 3. Finally, the model does not consider multiple cells close to one another, perturbing one another's fields. Nevertheless, none of these model assumptions will falsify the conclusions made in this paper. In fact, more detailed analysis on cellular non-homogeneity can only further clarify the impact of each aspect of the cell properties on electric field stimulation.

ACKNOWLEDGMENT

This work was supported by CIHR grants to PC and MGF, a Canadian Heart and Stroke Foundation (HSF) grant to MGF, and a HSF postdoctoral fellowship to Hui Ye.

APPENDIX A.

The solution of Laplace's equation in spherical coordinates can be expressed as [43]

$$V = \sum_{m,n} \left[\left(a_{nm} r^n + \frac{b_{nm}}{r^{n+1}} \right) \cos m\phi P_n^m(\cos\theta) + \left(c_{nm} r^n + \frac{d_{nm}}{r^{n+1}} \right) \sin m\phi P_n^m(\cos\theta) \right] \quad \text{(A1)}$$

where $P_n^m(\cos\theta)$ is the associated Legendre function ($n = 0 \ldots \infty$, $m = 0 \ldots n$). Since azimuthal symmetry is present for V, $m = 0$. Therefore, the solutions in the three different cell regions (Figure 1) are:

$$V_0 = \sum_{n=0}^{\infty} \left(a_n r^n + \frac{b_n}{r^{n+1}} \right) P_n(\cos\theta) \quad \text{(A2)}$$

$$V_0 = \sum_{n=0}^{\infty} \left(c_n r^n + \frac{d_n}{r^{n+1}} \right) P_n(\cos\theta) \quad \text{(A3)}$$

$$V_0 = \sum_{n=0}^{\infty} \left(e_n r^n + \frac{bf_n}{r^{n+1}} \right) P_n(\cos\theta) \quad \text{(A4)}$$

where a_n, b_n, c_n, d_n, e_n, f_n are undetermined coefficients ($n = 0, 1, 2$). V is continuous and bounded in all the considered regions and $P_n(\cos\theta)$ is the Legendre polynomial.

At an infinite distance, according to boundary condition (3), $V_0 = -Er\cos\theta = -ErP_1(\cos\theta)$. Therefore, $a_1 = -E$ and $a_n = 0 \quad (n \neq 1)$. $f_n = 0$ s***ince the potential inside the cell is finite*** (boundary condition 4). On the outer surface of the shell where $r = R_+$, $V_0 = V_1$ (boundary condition 1) and $S_0 \frac{\partial V_0}{\partial r} = S_1 \frac{\partial V_1}{\partial r}$ (boundary condition 2). Therefore,

$$-ER_+ P_1(\cos\theta) + \sum_{n=0}^{\infty} \frac{b_n}{R_+^{n+1}} P_n(\cos\theta) = \sum_{n=0}^{\infty} \left(c_n R_+^n + \frac{d_n}{R_+^{n+1}} \right) P_n(\cos\theta) \quad \text{(A5)}$$

$$-S_0\left[EP_1(\cos\theta)+\sum_{n=0}^{\infty}(n+1)\frac{b_n}{R_+^{n+2}}P_n(\cos\theta)\right]$$
$$=\ S_1\sum_{n=0}^{\infty}\left[nc_nR_+^{n-1}-(n+1)\frac{d_n}{R_+^{n+2}}\right]P_n(\cos\theta) \tag{A6}$$

Since $P_n(\cos\theta)$ are a complete set of orthogonal functions, the coefficients on both sides of (A5) and (A6) are equal. Therefore,

$$-ER_+ + \frac{b_1}{R_+^2} = c_1R_+ + \frac{d_1}{R_+^2} \tag{A7}$$

$$-S_o\left(E+\frac{2b_1}{R_+^3}\right) = S_1\left(c_1-\frac{2d_1}{R_+^3}\right) \tag{A8}$$

$$\frac{b_n}{R_+^{n+1}} = c_nR_+^n + \frac{d_n}{R_+^{n+1}} \quad (n\neq 1) \tag{A9}$$

$$-S_o(n+1)\frac{b_n}{R_+^{n+2}} = S_1\left[nc_nR_+^{n-1}-(n+1)\frac{d_n}{R_+^{n+2}}\right) \quad (n\neq 1) \tag{A10}$$

Similarly, on the inner surface of the shell where $r=R_-$, $V_1=V_2$ (boundary condition 1) and $S_1\frac{\partial V_1}{\partial r}=S_2\frac{\partial V_2}{\partial r}$ (boundary condition 2). Therefore,

$$c_1R_- + \frac{d_1}{R_-^2} = e_1R_- \tag{A11}$$

$$S_1\left(c_1-\frac{2d_1}{R_-^3}\right) = S_2e_1 \tag{A12}$$

$$c_nR_-^n + \frac{d_n}{R_-^{n+1}} = e_nR_-^n \quad (n\neq 1) \tag{A13}$$

$$S_2ne_nR_-^{n-1} = S_1\left[nc_nR_-^{n-1}-(n+1)\frac{d_n}{R_-^{n+2}}\right) \quad (n\neq 1) \tag{A14}$$

Solving Equations (A7) to (A14) yields

$$b_1 = ER_+^3\frac{(\sigma_1-\sigma_2)(2\sigma_1+\sigma_0)R_-^3+(2\sigma_1+\sigma_2)(\sigma_0-\sigma_1)R_+^3}{2(\sigma_1-\sigma_0)(\sigma_1-\sigma_2)R_-^3-(\sigma_1+2\sigma_0)(2\sigma_1+\sigma_2)R_+^3}$$

$$c_1 = E\frac{3\sigma_0(2\sigma_1+\sigma_2)R_+^3}{2(\sigma_1-\sigma_0)(\sigma_1-\sigma_2)R_-^3-(\sigma_1+2\sigma_0)(2\sigma_1+\sigma_2)R_+^3}$$

$$d_1 = E\frac{3\sigma_0(\sigma_1-\sigma_2)R_+^3R_-^3}{2(\sigma_1-\sigma_0)(\sigma_1-\sigma_2)R_-^3-(\sigma_1+2\sigma_0)(2\sigma_1+\sigma_2)R_+^3}$$

$$e_1 = E\frac{9\sigma_0\sigma_1 R_+^3}{2(\sigma_1-\sigma_0)(\sigma_1-\sigma_2)R_-^3-(\sigma_1+2\sigma_0)(2\sigma_1+\sigma_2)R_+^3}$$
$$b_n = c_n = d_n = e_n = 0 \quad (n \neq 1)$$

The potential distributions in the three regions are

$$V_0 = \left(\frac{1}{r^2}\frac{3\sigma_0(2\sigma_1+\sigma_2)R_+^6+3\sigma_0(\sigma_1-\sigma_2)R_+^3R_-^3}{2(\sigma_1-\sigma_0)(\sigma_1-\sigma_2)R_-^3-(\sigma_1+2\sigma_0)(2\sigma_1+\sigma_2)R_+^3} + \frac{R_+^3}{r^2} - r\right)E\cos\theta \quad \text{(A15)}$$

$$V_1 = \frac{3\sigma_0 R_+^3\left[r(2\sigma_1+\sigma_2)+(\sigma_1-\sigma_2)\frac{R_-^3}{r^2}\right]}{2(\sigma_1-\sigma_0)(\sigma_1-\sigma_2)R_-^3-(\sigma_1+2\sigma_0)(2\sigma_1+\sigma_2)R_+^3}E\cos\theta \quad \text{(A16)}$$

$$V_2 = \frac{9\sigma_0\sigma_1 R_+^3 r}{2(\sigma_1-\sigma_0)(\sigma_1-\sigma_2)R_-^3-(\sigma_1+2\sigma_0)(2\sigma_1+\sigma_2)R_+^3}E\cos\theta \quad \text{(A17)}$$

We further calculated the electric field distribution in the extracellular space, in the membrane, and in the cytoplasm, using

$$\vec{E} = -\nabla V = -\left(\frac{\partial V}{\partial r}, \frac{1}{r}\frac{\partial V}{\partial \theta}, \frac{1}{r\sin\theta}\frac{\partial V}{\partial \phi}\right) \quad \text{(A18)}$$

The expression derived for the electric field around the cell, in the extracellular medium (0#) was:

$$E_{0r} = \left[1+\frac{2R_+^3}{r^3}\frac{(\sigma_1-\sigma_2)(2\sigma_1+\sigma_0)R_-^3+(2\sigma_1+\sigma_2)(\sigma_0-\sigma_1)R_+^3}{2(\sigma_1-\sigma_0)(\sigma_1-\sigma_2)R_-^3-(\sigma_1+2\sigma_0)(2\sigma_1+\sigma_2)R_+^3}\right]E\cos\theta \quad \text{(A19)}$$

$$E_{0\theta} = \left[-1+\frac{R_+^3}{r^3}\frac{(\sigma_1-\sigma_2)(2\sigma_1+\sigma_0)R_-^3+(2\sigma_1+\sigma_2)(\sigma_0-\sigma_1)R_+^3}{2(\sigma_1-\sigma_0)(\sigma_1-\sigma_2)R_-^3-(\sigma_1+2\sigma_0)(2\sigma_1+\sigma_2)R_+^3}\right]E\sin\theta \quad \text{(A20)}$$

$$E_{0\phi} = 0 \quad \text{(A21)}$$

The expression derived for the membrane (1#) electric field was:

$$E_{1r} = \frac{6\sigma_0(\sigma_1-\sigma_2)R_-^3R_+^3/r^3-3\sigma_0(2\sigma_1+\sigma_2)R_+^3}{2(\sigma_1-\sigma_0)(\sigma_1-\sigma_2)R_-^3-(\sigma_1+2\sigma_0)(2\sigma_1+\sigma_2)R_+^3}E\cos\theta \quad \text{(A22)}$$

$$E_{1\theta} = \frac{3\sigma_0(\sigma_1-\sigma_2)R_-^3R_+^3/r^3+3\sigma_0(2\sigma_1+\sigma_2)R_+^3}{2(\sigma_1-\sigma_0)(\sigma_1-\sigma_2)R_-^3-(\sigma_1+2\sigma_0)(2\sigma_1+\sigma_2)R_+^3}E\sin\theta \quad \text{(A23)}$$

$$E_{1\phi} = 0 \quad \text{(A24)}$$

For Equations (A22) to (A24), if we let $r = R^-$, we obtained:

$$E_{1r} = \frac{9\sigma_0\sigma_2}{(\sigma_1+2\sigma_0)(2\sigma_1+\sigma_2)-2(\sigma_1-\sigma_0)(\sigma_1-\sigma_2)R_-^3/R_+^3}E\cos\theta \quad \text{(A25)}$$

$$E_{1\theta} = \frac{9\sigma_0\sigma_1}{(\sigma_1+2\sigma_0)(2\sigma_1+\sigma_2) - 2(\sigma_1-\sigma_0)(\sigma_1-\sigma_2)R_-^3/R_+^3} E\sin\theta \quad \text{(A26)}$$

$$E_{1\phi} = 0 \quad \text{(A27)}$$

The expression derived for the cytoplasmic electric field was:

$$E_{2r} = -\frac{9\sigma_0\sigma_1 R_+^3}{2(\sigma_1-\sigma_0)(\sigma_1-\sigma_2)R_-^3 - (\sigma_1+2\sigma_0)(2\sigma_1+\sigma_2)R_+^3} E\cos\theta \quad \text{(A28)}$$

$$E_{2\theta} = \frac{9\sigma_0\sigma_1 R_+^3}{2(\sigma_1-\sigma_0)(\sigma_1-\sigma_2)R_-^3 - (\sigma_1+2\sigma_0)(2\sigma_1+\sigma_2)R_+^3} E\sin\theta \quad \text{(A29)}$$

$$E_{2\phi} = 0 \quad \text{(A30)}$$

It is easy to validate Equations (A28) to (A30) by letting $\sigma_0 = \sigma_1 = \sigma_2$, the situation where there is no cell present in the external field. This yields $E_{2r} = E\cos\theta$ and $E_{2\theta} = -E\sin\theta$, respectively, which essentially is the unperturbed, externally applied, electric field.

REFERENCES

1. Gross, R. E. and A. M. Lozano, "Advances in neurostimulation for movement disorders," *Neurol. Res.*, Vol. 22, 247–58, Apr. 2000.
2. Ridding, M. C. and U. Ziemann, "Determinants of the induction of cortical plasticity by non-invasive brain stimulation in healthy subjects," *J. Physiol*, Vol. 588, 2291–2304, Jul. 1, 2010.
3. Chi, R. P. and A. W. Snyder, "Facilitate insight by non-invasive brain stimulation," *PLoS One*, Vol. 6, e16655, 2011.
4. Fedorov, A., Y. Chibisova, A. Szymaszek, M. Alexandrov, C. Gall, and B. A. Sabel, "Non-invasive alternating current stimulation induces recovery from stroke," *Restor. Neurol. Neurosci.*, Vol. 28, 825–833, 2010.
5. Lee, D. C. and W. M. Grill, "Polarization of a spherical cell in a nonuniform extracellular electric field," *Ann. Biomed. Eng.*, Vol. 33, 603–615, May 2005.
6. Kotnik, T. and D. Miklavcic, "Analytical description of transmembrane voltage induced by electric fields on spheroidal cells," *Biophys. J.*, Vol. 79, 670–679, Aug. 2000.
7. Fricke, H., "The electric permittivity of a dilute suspension of membrane-covered ellipsoids," *J. Appl. Phys.*, Vol. 24, 644–646, 1953.
8. Schwan, H. P., "Electrical properties of tissue and cell suspensions," *Adv. Biol. Med. Phys.*, Vol. 5, 147–209, 1957.

9. Kotnik, T., F. Bobanovic, and D. Miklavcic, "Sensitivity of transmembrane voltage induced by applied electric fields — A theoretical analysis," *Bioelectrochem. Bioenerg.*, Vol. 43, 285–291, 1997.
10. DeBruin, K. A. and W. Krassowska, "Modeling electroporation in a single cell. I. Effects of field strength and rest potential," *Biophys. J.*, Vol. 77, 1213–1224, Sep. 1999.
11. DeBruin, K. A. and W. Krassowska, "Modeling electroporation in a single cell. II. Effects of ionic concentrations," *Biophys. J.*, Vol. 77, 1225–1233, Sep. 1999.
12. Ye, H., M. Cotic, and P. L. Carlen, "Transmembrane potential induced in a spherical cell model under low-frequency magnetic stimulation," *J. Neural. Eng.*, Vol. 4, 283–293, Sep. 2007.
13. Gimsa, J. and D. Wachner, "Analytical description of the transmembrane voltage induced on arbitrarily oriented ellipsoidal and cylindrical cells," *Biophys. J.*, Vol. 81, 1888–1896, Oct. 2001.
14. Kotnik, T. and D. Miklavcic, "Theoretical evaluation of voltage inducement on internal membranes of biological cells exposed to electric fields," *Biophys. J.*, Vol. 90, 480–491, Jan. 15, 2006.
15. Pavlin, M., N. Pavselj, and D. Miklavcic, "Dependence of induced transmembrane potential on cell density, arrangement, and cell position inside a cell system," *IEEE Trans. Biomed. Eng.*, Vol. 49, 605–612, Jun. 2002.
16. Valic, B., M. Golzio, M. Pavlin, A. Schatz, C. Faurie, B. Gabriel, J. Teissie, M. P. Rols, and D. Miklavcic, "Effect of electric field induced transmembrane potential on spheroidal cells: Theory and experiment," *Eur. Biophys. J.*, Vol. 32, 519–528, Sep. 2003.
17. Farkas, D. L., R. Korenstein, and S. Malkin, "Electrophotoluminescence and the electrical properties of the photosynthetic membrane. I. Initial kinetics and the charging capacitance of the membrane," *Biophys. J.*, Vol. 45, 363–373, Feb. 1984.
18. Jerry, R. A., A. S. Popel, and W. E. Brownell, "Potential distribution for a spheroidal cell having a conductive membrane in an electric field," *IEEE Trans. Biomed. Eng.*, Vol. 43, 970–972, Sep. 1996.
19. Wachner, D., M. Simeonova, and J. Gimsa, "Estimating the subcellular absorption of electric field energy: Equations for an ellipsoidal single shell model," *Bioelectrochemistry*, Vol. 56, 211–213, May 15, 2002.
20. Faber, D. S. and H. Korn, "Field effects trigger post-anodal rebound excitation in vertebrate CNS," *Nature*, Vol. 305, 802–

804, Oct. 27–Nov. 2, 1983.

21. Dudek, F. E., T. Yasumura, and J. E. Rash, "'Non-synaptic' mechanisms in seizures and epileptogenesis," *Cell Biol. Int.*, Vol. 22, 793–805, Nov. 1998.
22. Rattay, F., "Analysis of the electrical excitation of CNS neurons," *IEEE Trans. Biomed. Eng.*, Vol. 45, 766–772, Jun. 1998.
23. McIntyre, C. C., W. M. Grill, D. L. Sherman, and N. V. Thakor, "Cellular effects of deep brain stimulation: Model-based analysis of activation and inhibition," *J. Neurophysiol.*, Vol. 91, 1457–1469, Apr. 2004.
24. Gimsa, U., U. Schreiber, B. Habel, J. Flehr, U. van Rienen, and J. Gimsa, "Matching geometry and stimulation parameters of electrodes for deep brain stimulation experiments — Numerical considerations," *J. Neurosci. Methods*, Vol. 150, 212–227, Jan. 30, 2006.
25. Sukharev, S. I., V. A. Klenchin, S. M. Serov, L. V. Chernomordik, and A. Chizmadzhev Yu, "Electroporation and electrophoretic DNA transfer into cells. The effect of DNA interaction with electropores," *Biophys. J.*, Vol. 63, 1320–1327, Nov. 1992.
26. Kinosita, Jr., K. and T. Y. Tsong, "Voltage-induced pore formation and hemolysis of human erythrocytes," *Biochim. Biophys. Acta*, Vol. 471, 227–242, Dec. 1, 1977.
27. Somiari, S., J. Glasspool-Malone, J. J. Drabick, R. A. Gilbert, R. Heller, M. J. Jaroszeski, and R. W. Malone, "Theory and in vivo application of electroporative gene delivery," *Mol. Ther.*, Vol. 2, 178–187, Sep. 2000.
28. Yousif, N., R. Bayford, and X. Liu, "Revealing the biophysical mechanism for configuring electrode contacts in deep brain stimulation," *Sixteenth Annual Computational Neuroscience Meeting: CNS*2007*, P143, Toronto, Canada, 2007.
29. Mossop, B. J., R. C. Barr, J. W. Henshaw, and F. Yuan, "Electric fields around and within single cells during electroporation-a model study," *Ann. Biomed. Eng.*, Vol. 35, 1264–1275, Jul. 2007.
30. Mossop, B. J., R. C. Barr, D. A. Zaharoff, and F. Yuan, "Electric fields within cells as a function of membrane resistivity — A model study," *IEEE Trans. Nanobioscience*, Vol. 3, 225–231, Sep. 2004.
31. Bryant, G. and J. Wolfe, "Electromechanical stresses produced in the plasma membranes of suspended cells by applied electric fields," *J. Membr. Biol.*, Vol. 96, 129–139, 1987.
32. Pucihar, G., T. Kotnik, B. Valic, and D. Miklavcic, "Numerical determination of transmembrane voltage induced on irregularly

shaped cells," *Ann.Biomed. Eng.*, Vol. 34, 642–652, Apr. 2006.

33. Vigmond, E. J., J. L. Perez Velazquez, T. A. Valiante, B. L. Bardakjian, and P. L. Carlen, "Mechanisms of electrical coupling between pyramidal cells," *J. Neurophysiol*, Vol. 78, 3107–3116, Dec. 1997.
34. Loew, L. M., "Voltage-sensitive dyes: Measurement of membrane potentials induced by DC and AC electric fields," *Bioelectromagnetics*, Vol. 1, 179–189, 1992.
35. Ghai, R. S., M. Bikson, and D. M. Durand, "Effects of applied electric fields on low-calcium epileptiform activity in the CA1 region of rat hippocampal slices," *J. Neurophysiol*, Vol. 84, 274–280, Jul. 2000.
36. Grill, Jr., W. M., "Modeling the effects of electric fields on nerve fibers: Influence of tissue electrical properties," *IEEE Trans. Biomed. Eng.*, Vol. 46, 918–928, Aug. 1999.
37. Sotiropoulos, S. N. and P. N. Steinmetz, "Assessing the direct effects of deep brain stimulation using embedded axon models," *J. Neural. Eng.*, Vol. 4, 107–119, Jun. 2007.
38. Gehl, J., "Electroporation: Theory and methods, perspectives for drug delivery, gene therapy and research," *Acta Physiol. Scand.*, Vol. 177, 437–447, Apr. 2003.
39. Ehrenberg, B., D. L. Farkas, E. N. Fluhler, Z. Lojewska, and L. M. Loew, "Membrane potential induced by external electric field pulses can be followed with a potentiometric dye," *Biophys. J.*, Vol. 51, 833–837, May 1987.
40. Teruel, M. N. and T. Meyer, "Electroporation-induced formation of individual calcium entry sites in the cell body and processes of adherent cells," *Biophys. J.*, Vol. 73, 1785–1796, Oct. 1997.
41. Holsheimer, J., "Electrical conductivity of the hippocampal CA1 layers and application to current-source-density analysis," *Exp. Brain Res.*, Vol. 67, 402–410, 1987.
42. Tyner, K. M., R. Kopelman, and M. A. Philbert, "'Nanosized voltmeter enables cellular-wide electric field mapping," *Biophys. J.*, Vol. 93, 1163–1174, Aug. 15, 2007.
43. Stratton, J. A., *Electromagnetic Theory*, McGraw-Hill, New York, 1941.